

See discussions, stats, and author profiles for this publication at: <https://www.researchgate.net/publication/231706029>

# pH-Controllable Depletion Attraction Induced by Microgel Particles

ARTICLE *in* MACROMOLECULES · OCTOBER 2009

Impact Factor: 5.8 · DOI: 10.1021/ma901130x

---

CITATIONS

16

---

READS

22

3 AUTHORS, INCLUDING:



Zifu Li

Georgia Institute of Technology

25 PUBLICATIONS 372 CITATIONS

SEE PROFILE



To Ngai

The Chinese University of Hong Kong

94 PUBLICATIONS 1,304 CITATIONS

SEE PROFILE

## pH-Controllable Depletion Attraction Induced by Microgel Particles

Xiaochen Xing, Zifu Li, and To Ngai\*

Department of Chemistry, The Chinese University of Hong Kong, Shatin, N.T., Hong Kong

Received May 24, 2009

Revised Manuscript Received August 31, 2009

Entropic depletion attractions between colloidal particles are ubiquitous and arise solely from physical considerations of excluded volume. In a mixture of large colloidal particles and nonadsorbed nanoscale particles (often known as depletants), when the surfaces of two large particles happen to approach within the diameter  $d$  of the nanoscale particles, the smaller particles can be excluded from the region between the two larger particles, thereby creating an attractive force between the two larger particles due to an imbalance osmotic pressure ( $\Pi$ ) inside and outside the gap region.<sup>1</sup> The entropic depletion force has been the subject of several studies over the past decade because it plays an important role in many industrial applications.<sup>2</sup> In addition, such force is also involved in controlling biological interactions,<sup>3–5</sup> in organizing self-assembly of colloidal suspensions,<sup>6–8</sup> and in the creation of complex materials.<sup>9,10</sup> For examples, Mason has used depletion forces for disk-shaped particles to direct the assembly of stacks of clay disks,<sup>11</sup> Stroock and co-workers have similarly used depletion forces to assemble short cylinders with flat ends,<sup>12</sup> and Dinsmore et al.<sup>13</sup> have applied depletion forces to sort particles onto fated surfaces. One advantage in using depletion forces for assembly is that the interaction potentials are easily controlled in the weak-attraction regime, namely,  $1–5 k_B T$ .

Theoretical progress on the depletion problem began in the late 1950s. Asakura and Oosawa (AO)<sup>14</sup> and Vrij<sup>15</sup> independently calculated the depletion potential between two colloidal particles in ideal dilute polymer solutions. They treated colloidal particles as hard spheres and assumed that an ideal polymer chain was a penetrable hard sphere to another polymer chain but was impenetrable for colloidal particles. Using this model, they obtained a simple depletion potential with a range of the radius of gyration of polymer ( $R_g$ ) and strength proportional to the concentration of polymers. Despite its simplicity, AO theory captures the length scale and magnitude of the entropy-driven depletion force in fair agreement with simulations and experiments. The experimental investigations of depletion interactions have been conducted in the presence of nonadsorbing nanoparticle suspensions,<sup>16</sup> surfactant micellar solutions,<sup>17,18</sup> polymer solutions,<sup>19,20</sup> and charged polyelectrolytes.<sup>21,22</sup>

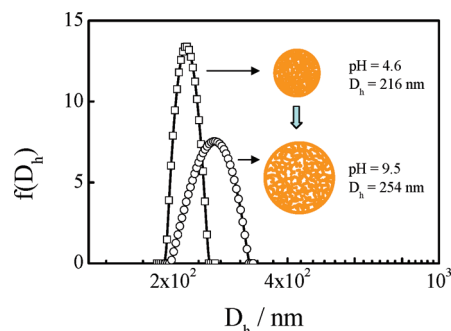
However, it is worth mentioning that most experimental studies of depletion interactions have been indirect or limited in scope. Direct measurements of depletion interactions are still experimentally challenging, if not impossible, as they require the detection of potential variations of the order of  $k_B T$  and beyond.<sup>23</sup> Unsurprisingly, depletion was first measured directly only 17 years ago using the surface force apparatus (SFA).<sup>17</sup> Measurements have recently become possible with the improved sensitivity afforded by techniques such as optical tweezers (OT),<sup>24–26</sup>

atomic force microscopy (AFM),<sup>27,28</sup> and total internal reflection microscope (TIRM).<sup>29–31</sup> In particular, TIRM is an extremely sensitive noninvasive technique that has been used to catch the weak depletion force acting on a free-moving particle in the presence of neutral polymer,<sup>32</sup> charged colloidal rods,<sup>33</sup> or even nanobubbles.<sup>34,35</sup>

In this work, we present the first study of the depletion potentials of a free colloidal sphere close to a wall in the presence of poly(*N*-isopropylacrylamide-*co*-methacrylic) (PNIPAM-*co*-MAA) microgel particles. One advantage of using PNIPAM-*co*-MAA microgel particles as the depleting agents lies in the fact that PNIPAM-based microgels exhibit an extreme response to changes in pH, which can lead to dramatic changes in particle size. We found that the depletion interactions can be easily triggered by changing the pH values of the solution containing microgel particles and thus provide a new way of using depletion forces to direct the assembly of colloidal particles.

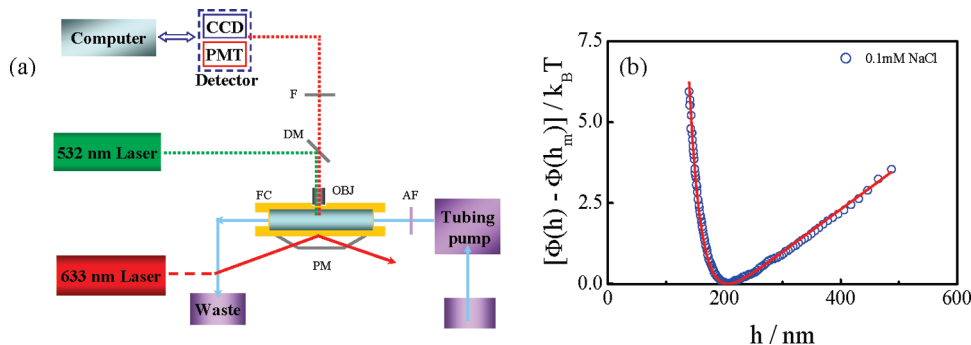
The PNIPAM-*co*-MAA microgels with low polydispersity were synthesized via emulsion polymerization without using surfactants.<sup>36,37</sup> The incorporation of MAA allows generation of internal charges at a pH value greater than 6 ( $pK_a \approx 6.2$ ), which leads to increased osmotic pressure and thus swelling of the microgels. Figure 1 confirms the pH-responsive behavior of the synthesized microgel particles. The hydrodynamic diameter of PNIPAM-*co*-MAA microgels increases from 216 to 254 nm when solution pH is increased from 4.6 to 9.5.<sup>37</sup> Note that PNIPAM-based microgels are also well-known to undergo the volume phase transition by change of temperature,<sup>36</sup> and recently, such temperature-dependent hydrogels have been employed as depletants to thermoreversibly tune colloidal attraction<sup>38</sup> and interfacial colloidal crystallization.<sup>39</sup> However, for our synthesized microgels, we observed a very broad temperature change accompanied by small shrinkage in volume at both pH 4.6 and 9.5. The reason for the broad temperature and small volume transition may be related to the inhomogeneous distribution of the comonomer in the PNIPAM-*co*-MAA copolymer microgels particularly with low MAA content.<sup>36</sup> Thus, in this study, we will only investigate the effect of pH-triggered volume phase transition of the PNIPAM-*co*-MAA microgel particles on the interaction potentials between the sphere and flat surface by means of TIRM.

Figure 2a shows our TIRM setup used to measure the pH-triggered depletion potentials between a free-moving polystyrene (PS) sphere and a hydrophilic glass surface in the presence of PNIPAM-*co*-MAA microgels. TIRM uses evanescent



**Figure 1.** pH dependence of the hydrodynamic diameter ( $D_h$ ) of PNIPAM-*co*-MAA microgels in an aqueous dispersion with microgel concentration of  $10^{-5}$  g/mL at room temperature.

\*To whom correspondence should be addressed. E-mail: tongai@cuhk.edu.hk.



**Figure 2.** (a) Experimental setup used to directly measure the interaction between the polystyrene sphere and flat surface before and after introducing the PNIPAM-*co*-MAA microgels, where FC = flow cell, PM = prism, and OBJ = objective. (b) Typical interaction potential between a charged PS sphere and a charged surface in 0.1 mM NaCl aqueous solution. The solid line is a theoretical fitted curve from eq 1.

wave light scattered by a single sphere near a flat surface to determine the equilibrium distribution of sphere–surface separations and the associated interaction energy. The details of this technique have been described elsewhere.<sup>29,32,34</sup> In the TIRM force measurements, a very diluted PS dispersion in 0.1 mM NaCl solution was initially filled into a sample cell sandwiched between two silica microscopy slides. The slides were cleaned by following the normal procedures as described before.<sup>34,35</sup> A PS sphere of average brightness was selected and held in place with optical tweezers by a solid-state Nd:YAG laser (output = 300 mW at wavelength = 532 nm), while the rest of the spheres were flushed from the cell with NaCl aqueous solution. Once the excess spheres were washed away, the interaction potential between the single free-moving sphere and bare glass surface in 0.1 mM NaCl solution was recorded. Figure 2b shows that the interaction potential of the negatively charged PS sphere at height  $h$  above the glass plate is composed of two parts: toward larger  $h$  the potential increases linearly because the dominant force acting on the particle is gravity. At smaller  $h$  the potential increases exponentially because of the electrostatic interaction between the negatively charged particle and also the negatively charged silica surface. In this case the interaction potential between the sphere and surface can be described as<sup>29,34</sup>

$$\frac{\Phi(h)}{k_B T} = B e^{-\kappa h} + \frac{G}{k_B T} h \quad (1)$$

where the amplitude of the electrostatic interaction  $B$  depends on the surface charges of the particle and the silica surface,  $\kappa^{-1}$  is Debye screening length of the solvent, and  $G$  is the weight of the particle. The solid line in the figure shows that the measured potential is well described by eq 1, which also experimentally confirmed by several groups using TIRM.<sup>29,30,33</sup>

After measuring the interaction potential in pure NaCl solution, ~20 mL of deionized water was first used to rinse the sample cell and PNIPAM-*co*-MAA microgel dispersions with different concentrations at pH 9.43 (adjusted by NaOH) were then subsequently pumped into the cell by a flex tubing pump (Master Flex), while the PS sphere was trapped in place by tweezers. The trapped sphere was then released, and the interaction potentials between the sphere and surface were measured in the presence of different concentrations of swollen microgel particles. It is worthy to point out that the consecutive potentials are measured with the same PS sphere and same surface before and after introducing the microgels; thus, we can isolate the effect of existing microgels in the solution by the comparison among measured potentials.

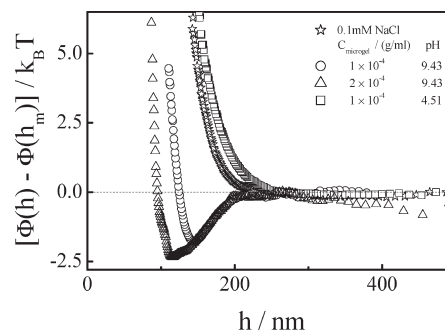


**Figure 3.** Measured interaction potentials ( $\Phi(h)/k_B T$ ) between the polystyrene sphere and flat surface under different environmental conditions, namely, in 0.1 mM NaCl aqueous solution, in different concentrations of microgel dispersion at pH = 9.43, and in microgel dispersion at pH = 4.51. Note that the gravity of all the interaction potentials has been subtracted.

Figure 3 shows that the interaction potentials between the PS sphere and surface in the presence of swollen microgels are significantly changed. Note that the contribution of gravity has been subtracted from all potentials since the same PS sphere was used. It clearly shows that the addition of swollen microgels induces a long-range attractive force occurring at separation distances ranging from 150 to 250 nm, which may be contributed to either bridging or depletion. This attractive force is seen to increase with increasing swollen microgel concentration, while the separation distance decreases. Moreover, at higher swollen microgel volume fractions, the attractive well becomes narrow and steep as well as acting over smaller separation distances. It is expected that the microgels at pH 9.43 are negatively charged due to the dissociation of  $-\text{COOH}$  on the network chains. The selected PS sphere and the hydrophilic glass surface are also negatively charged during the measurements. Thus, we can reasonably assume that microgels will not preferentially absorb to either the PS sphere or glass surface and exclude the bridging effect. One may wonder whether the measured attractive force is due to the alternation of the electrostatic interaction between the PS sphere and the flat surface after introducing the microgels. To answer this question, we first measured the conductivity ( $19 \pm 0.2 \mu\text{S cm}^{-1}$ ) of microgel dispersion with concentration  $1 \times 10^{-4} \text{ g/mL}$  at pH 9.43 and found that it was the same as a 0.1 mM NaCl aqueous solution. That means ionic strength or Debye length of the aqueous solution is similar before and after introducing the microgels. The only different between the two solutions is the presence of microgels or not. To have an even clearer picture, we further calculated the surface potential between the PS sphere and the surface in the aqueous solution

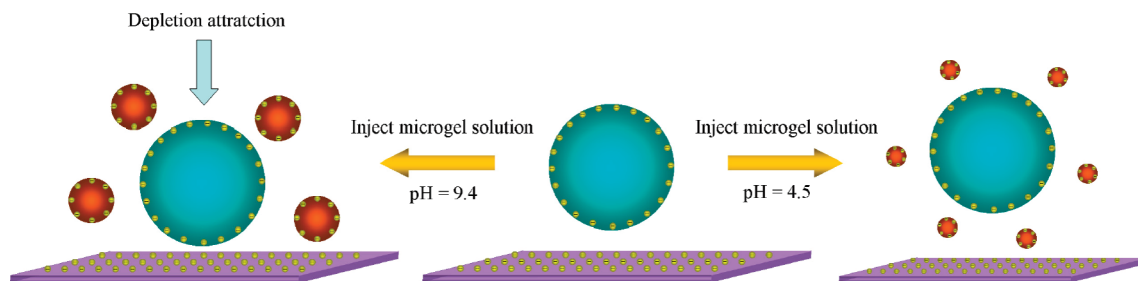


**Figure 4.** Schematic shows the pH-triggered depletion attraction acting on polystyrene sphere immersed in the microgel dispersion close to a flat surface.

by applying eq 1 to fit the measured potential profiles before and after introducing the swollen microgels. The fitting provides two parameters, namely,  $\kappa^{-1}$  and  $G$ . Note that in eq 1  $\Phi(h)$  has a minimum at a separation distance  $h_m$  given by<sup>29</sup>

$$\kappa h_m = \ln \frac{\kappa B}{G} \quad (2)$$

where  $h_m$  can be directly read from the measured potentials as shown in Figure 3. In this way, we can find the constant  $B$  which reflects the electrostatic repulsion potential between the two surfaces.<sup>29,35</sup> The values of  $\ln B$  in 0.1 mM NaCl solution and microgel dispersion with pH 9.43 were determined as 9.0 and 13.1, respectively, indicating that the surface repulsion increases in the presence of swollen microgels. In other words, the separation distance between the PS sphere and surface is expected to be larger. However, it can be seen from Figure 3 that our measured interaction potentials shift to a smaller distance in the presence of microgels. We therefore suggest that the measured attractive force is likely caused by the exclusion or depletion of the large swollen microgels from the gap between the PS sphere and the surface. At 0.1 mM NaCl solution, the separation distance between the sphere–surface ( $\sim 220$  nm) is smaller than the hydrodynamic diameter of the swollen microgels ( $\sim 254$  nm) under the condition of pH 9.43. The exclusion results in an osmotic pressure imbalance inside and outside the gap region, leading to the net attraction.

Increasing the microgel concentration from  $1 \times 10^{-4}$  to  $2 \times 10^{-4}$  g/mol increases the magnitude of this attractive force. As a result, the measured potential energy profiles become narrower and shifts to smaller separation distances. However, the wall depth of the measured potential energy files has not doubled as expected. One of reasons may be due to the fact that the concentration of microgel particles used is not in the dilute limit. Second, some recent studies have suggested that long-range electrostatic repulsion between the charge depleting agents could significantly affect the magnitude and range of the depletion attraction.<sup>18,20</sup> The depletion interaction in semidilute and concentrated solutions will need to be closely examined in the future.

As mentioned above, the hydrodynamic volume of microgels can respond to pH changes; one might expect the measured depletion attractive force to be a function of pH, too. To confirm such hypothesized pH dependence, we rinsed the sample cell with a large amount of deionized water (changing the volume inside the cell at least 20 times) and then pumped the microgels with solution pH 4.51. Figure 3 shows that the measured long-range attractive force disappears, leaving only the electrostatic repulsion. We related this effect to the collapsed microgels, with the hydrodynamic diameter smaller than the sphere–surface distance, which are able to move into the gap region. The imbalance in osmotic pressure inside and outside the region will disappear as will the depletion attractive force. Note that this attractive force can be regenerated by reintroduction of microgels at high pH condition, and the process is reversible, which in turn indicates

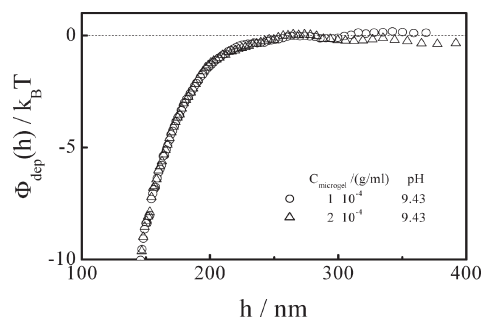


**Figure 5.** Measured depletion potentials between the polystyrene sphere and the flat surface in the presence of different amounts of swollen microgels.

that microgel-triggered depletion attractive force is pH dependent as schematically summarized in Figure 4.

To isolate the microgel-induced depletion potential and compare to theoretical mode, each measured potential at pH 9.43 was subtracted by the potential at pH 4.51. The net depletion interactions were obtained and plotted in Figure 5. It clearly shows that the depletion attraction is continuous and with the measurable distance up to  $\sim 250$  nm. The classical depletion potential function was used to fit the measured profiles shown in Figure 5, namely

$$\Phi_{\text{dep}}(h) = \begin{cases} -\pi\Pi \left[ (a+\Delta)(h-2\Delta)^2 + \frac{1}{3}(h-2\Delta)^3 \right] & \text{for } 0 < h < 2\Delta \\ 0 & \text{for } h > 2\Delta \end{cases} \quad (3)$$

where  $\Pi$  is the osmotic pressure of the bulk solution,  $a$  is the radius of the polystyrene particle (here  $a = 3.0 \mu\text{m}$ ), and  $2\Delta$  is the depletion region.<sup>40</sup> The fitting gives  $2\Delta \sim 250$  nm and  $\Pi \sim 0.4$  Pa. Note that the fitted depletion region can be compared to the hydrodynamic diameter of the swollen microgels, suggesting that our experimental results are in good agreement with the theoretical values predicated by eq 3.

In summary, we report the first direct measurement of the pH-triggered depletion interaction potentials between a polystyrene sphere and a flat substrate as mediated by PNIPAM-*co*-MAA microgels. When the solution pH of the microgel dispersion was high, an attractive force occurring at separation distance of 150–250 nm was observed and increased in magnitude with increasing microgel concentrations. The origin of this attractive force comes from exclusion or depletion of large swollen microgels between the PS particle and flat surface and is affected by the electrostatic interactions between the microgel particles. However, this depletion force disappeared upon changing the microgel dispersion to a low-pH solution. The current study demonstrates the ability to quantitatively measure and reversibly control  $k_B T$ -scale depletion attraction as a function of solution pH.

Therefore, it offers a promising route to use such tunable depletion forces in the formation of complex colloidal assemblies.

**Acknowledgment.** The financial support of this work by the Hong Kong Special Administration Region (HKSAR) Earmarked Project (CUHK402506, 2160291) is gratefully acknowledged.

## References and Notes

- (1) Tuinier, R.; Rieger, J.; de Kruit, C. G. *Adv. Colloid Interface Sci.* **2003**, *103*, 1.
- (2) Farinato, R. S.; Dubin, P. L. Eds. *Colloid-Polymer Interactions: From Fundamentals to Practice*; Wiley-VCH: New York, 1999.
- (3) Poon, W. C. K. *J. Phys.: Condens. Matter* **2002**, *14*, R859.
- (4) Mutch, K. J.; van Duijneveldt, J. S.; Eastoe, J. *Soft Matter* **2007**, *3*, 155.
- (5) Snir, Y.; Kamien, R. D. *Science* **2005**, *307*, 1067.
- (6) Kaplan, P. D.; Rouke, J. L.; Yodh, A. G. *Phys. Rev. Lett.* **1994**, *72*, 582.
- (7) Dinsmore, A. D.; Yodh, A. G.; Pine, D. J. *Nature* **1996**, *383*, 239.
- (8) Lin, K.-H.; Crocker, J. C.; Prasad, V.; Schofield, A.; Weitz, D. A.; Lubensky, T. C.; Yodh, A. G. *Phys. Rev. Lett.* **2000**, *85*, 1770.
- (9) Wilking, J. N.; Graves, S. M.; Chang, B. C.; Meleson, K.; Lin, M. Y.; Mason, T. G. *Phys. Rev. Lett.* **2006**, *96*, 015501.
- (10) Dinsmore, A. D.; Prasad, V.; Wong, I. Y.; Weitz, D. A. *Phys. Rev. Lett.* **2006**, *96*, 185502.
- (11) Mason, T. G. *Phys. Rev. E* **2002**, *66*, 060402.
- (12) Badaire, S.; Cottin-Bizonne, C.; Woody, J. W.; Yang, A.; Stroock, A. D. *J. Am. Chem. Soc.* **2007**, *129*, 40.
- (13) Dinsmore, A. D.; Yodh, A. G. *Langmuir* **1999**, *15*, 314.
- (14) Asakura, S.; Oosawa, F. *J. Chem. Phys.* **1954**, *22*, 1255.
- (15) Vrij, A. *Pure Appl. Chem.* **1976**, *48*, 471.
- (16) Sharma, A.; Walz, J. Y. *J. Chem. Soc., Faraday Trans.* **1996**, *92*, 4997.
- (17) Richetti, P.; Kekicheff, P. *Phys. Rev. Lett.* **1992**, *68*, 1951.
- (18) Sober, D. L.; Walz, J. Y. *Langmuir* **1995**, *11*, 2352.
- (19) Milling, A. J.; Kendall, K. *Langmuir* **2000**, *16*, 5106.
- (20) Piech, M.; Walz, J. Y. *J. Phys. Chem. B* **2004**, *108*, 9177.
- (21) Biggs, S.; Dagastine, R. R.; Prieve, D. C. *J. Phys. Chem. B* **2002**, *106*, 11557.
- (22) Biggs, S.; Prieve, D. C.; Dagastine, R. R. *Langmuir* **2005**, *21*, 5421.
- (23) Kleshchanok, D.; Tuinier, R.; Lang, P. R. *J. Phys.: Condens. Matter* **2008**, *20*, 073101.
- (24) Verma, R.; Crocker, J. C.; Lubensky, T. C.; Yodh, A. G. *Phys. Rev. Lett.* **1998**, *81*, 4004.
- (25) Crocker, J. C.; Matteo, J. A.; Dinsmore, A. D.; Yodh, A. G. *Phys. Rev. Lett.* **1999**, *82*, 4352.
- (26) Lin, K.-H.; Crocker, J. C.; Zeri, A. C.; Yodh, A. G. *Phys. Rev. Lett.* **2001**, *87*, 088301.
- (27) Milling, A. J.; Biggs, S. J. *Colloid Interface Sci.* **1995**, *170*, 604.
- (28) Knoben, W.; Besseling, N. A. M.; Cohen Stuart, M. A. *Phys. Rev. Lett.* **2006**, *97*, 06830.
- (29) Prieve, D. C. *Adv. Colloid Interface Sci.* **1999**, *82*, 93.
- (30) Kleshchanok, D.; Lang, P. R. *Langmuir* **2007**, *23*, 4332.
- (31) Hertlein, C.; Helden, L.; Gambassi, A.; Dietrich, S.; Bechinger, C. *Nature* **2008**, *451*, 172.
- (32) Rudhardt, D.; Bechinger, C.; Leiderer, P. *Phys. Rev. Lett.* **1999**, *81*, 1330.
- (33) Helden, L.; Koenderink, G. H.; Leiderer, P.; Bechinger, C. *Langmuir* **2004**, *20*, 5662.
- (34) Jin, F.; Gong, X. J.; Ye, J.; Ngai, T. *Soft Matter* **2008**, *4*, 968.
- (35) Ngai, T.; Xing, X. C.; Jin, F. *Langmuir* **2008**, *24*, 13912.
- (36) Zhou, S. Q.; Chu, B. *J. Phys. Chem. B* **1998**, *102*, 1364.
- (37) Ngai, T.; Auweter, H.; Behrens, S. H. *Macromolecules* **2006**, *39*, 8171.
- (38) Savage, T. R.; Blair, D. W.; Levine, A. J.; Guyer, R. A.; Dinsmore, A. D. *Science* **2006**, *314*, 795.
- (39) Fernandes, G. E.; Beltran-Villegas, D. J.; Bevan, M. A. *Langmuir* **2008**, *24*, 10776.
- (40) Scheutjens, J. M. H. M.; Fleer, G. J. *J. Phys. Chem.* **1979**, *83*, 1619; **1980**, *84*, 178.